Proceedings of the ASME 2010 3rd Joint US-European Fluids Engineering Summer Meeting and 8th International Conference on Nanochannels, Microchannels, and Minichannels
FEDSM-ICNMM2010
August 1-5, 2010, Montreal, Canada

FEDSM-ICNMM2010-30378

EFFECTS OF ROLLING ANGULAR VELOCITY ON THE FLUTTER OF WING-STORE UNDER FOLLOWER FORCE

A. Mazidi
Shiraz University
Shiraz, I.R. Iran

S. A. Fazelzadeh
Shiraz University
Shiraz, I.R. Iran

P. Marzocca
Clarkson University
Potsdam, USA

ABSTRACT

The flutter analysis of a swept aircraft wing-store configuration subjected to follower force and undergoing a roll maneuver is presented. Concentrated mass, follower force, and roll angular velocity terms are combined in the governing equations which are obtained using the Hamilton's principle. The wing is modeled from a classical beam theory and incorporates bending-torsion flexibility. Heaviside and Dirac delta functions are used to consider the location and properties of the external mass and the follower force. Also, Peter's unsteady aerodynamic pressure loadings are considered and modified to take the wing sweep angle effect into account. The Galerkin method is applied to convert the partial differential equations into a set of ordinary differential equations. Numerical simulations are validated with available published results. In addition, simulation results are presented to show the effects of the roll angular velocity, sweep angle, follower force, and engine mass and location, on the wing flutter. Results are indicative of the significant effect of the rigid body roll angular velocity and the follower force on the wing-engine dynamic stability. Furthermore, distances between the engine center of gravity and the wing elastic axis contribute considerable effects in the wing-engine flutter speed and frequency.

INTRODUCTION

Civil and military airplane wings are subjected to a variety of non-conservative forces, such as aeroelastic forces, maneuver loads, and follower forces. Since rigid body rotations due to maneuver angular velocities, such as the one produced by a roll maneuver, can adversely affect the aircraft aeroelastic stability region, it is critical to include maneuvering angular velocities in aeroelastic analysis. Furthermore, a wide variety of external stores, such as heavy engine nacelles, in the case of transport aircraft, or missiles, for military aircrafts, are usually present in typical modern aircraft configuration. The geometrical and physical parameters of such external stores have a complex influence on the flutter characteristics of aircraft wings, primarily because of the store inertial and elastic coupling effect with the wing. Also, modern aircraft wings are usually subjected to several types of follower forces, for example produced by jet propulsion, rocket thrusts, thermal loading, only to name a few. The interaction between follower forces and aerodynamics, particularly for wing-store configurations, has important effects on the aeroelastic stability of the aircraft. Therefore, for a reliable aeroelastic analysis of aircraft wings it is necessary to develop refined simulation models and tools to account for the effects of external stores, follower forces and maneuver angular velocities, and all conditions need to be considered simultaneously.

The wing aeroelasticity is an old and practical problem and numerous papers have been published in this field, too many to list them all. Only a few relevant contributions will be discussed next. One of the first research contributions is the paper by Goland [1] on the determination of the flutter speed for a uniform cantilever wing by integration of the differential equations of the wing motion. An extension was provided for a uniform wing with tip weights [2]. Harry and Charlz [3] analyzed the flutter of a uniform wing and made a comparison between the analytical and the experimental results. The aeroelastic stability of a swept wing with tip weights for an unrestrained vehicle has been considered by Lottati [4]. In his work a composite wing was studied and it was observed that flutter occurs at a lower speed as compared with a clean wing configuration. Gern and Librescu contributed to show the effects of externally mounted stores on the static and dynamic aeroelasticity of advanced swept cantilevered wings [5, 6]. The dynamic response of adaptive cantilevered beams carrying externally mounted stores and exposed to time-dependent external excitations has been considered by Na and Librescu [7]. Moreover, Librescu and Song [8] investigated the free vibration and dynamic response to external time-dependent loads of aircraft wings carrying eccentrically located heavy stores. In these contributions the authors have modeled the wing as a thin-walled anisotropic composite beam.

Follower forces are frequently encountered in structural engineering, and they can be either static or dynamic. Bolotin [9] provided a general understanding of the effect of non-conservative forces on elastic systems. The lateral stability of a beam under the transverse follower force was analyzed first for a pinned configuration. The correlation between stability and quasi stability regions of elastic and viscoelastic systems subjected to non-conservative forces was investigated by Bolotin and Zhinzher [10]. The equations for a cantilevered thin beam were derived by Kalmbach et al [11]. They examined the possibility of controlling, through feedback, a thin-cantilevered beam subjected to a non-conservative follower force. The static and dynamic instabilities of a cantilevered beam and a simply supported plate under non-conservative forces have been studied by Zuo and Schreyer [12]. For the beam model the governing partial differential equation and associated boundary conditions of the continuous model have been solved exactly. Detinko [13] used a simple model of a slender beam loaded by a transverse follower force to show that the lateral stability analysis of a beam under the follower load should include realistic amount damping to reach a correct evaluation of the critical load.

In these contributions the effects of transverse follower forces on the elastic stability of the structures have been studied. However, much of the research in this field is on the stability of the structures subjected to different types of follower forces and there is very little literature concerned with the aeroelastic stability of such structures. It seems that the stability problem of a cantilever wing containing a mass excited by a transverse follower force and subjected to aerodynamic loads has not received much attention in the literature. Como [14] analyzed the bending-torsional stability of a cantilevered beam subjected at its end section to a lateral follower force. The distributed mass and inertia properties of the beam were neglected, although a concentrated mass and inertia at the tip were included. Feldt and Herrmann [15] investigated the flutter instability of a wing containing a mass subjected to the transverse follower force at the wing tip in the presence of airflow. Only one value of the bending stiffness to torsional stiffness ratio was considered in their study, a value for which thrust is destabilizing. Their results generally did not agree with previous works. Hodges et al have shown the effects of the lateral follower force on flutter boundary and frequency of cantilever wings [16, 17]; however, they did not take into account the external concentrated mass effects. The bending-torsional flutter characteristics of an un-swept wing containing an arbitrarily placed mass under a follower force have been studied by Fazelzadeh et al [18]. The Theodorsen unsteady aerodynamic model is used for flutter analysis. The important influence of the location and magnitude of the mass and the follower force on the flutter speed and frequency of the un-swept wing was highlighted. In a subsequent work Mazidi and Fazelzadeh [19] emphasized the effects of the wing sweep angle on the flutter boundaries.

In high-speed advanced flight vehicles some non-conservative terms in aeroelastic governing equations are caused by complex maneuvering conditions. The effect of the aircraft maneuvers on the wing instability has not been thoroughly investigated. Nonlinear equations of motion for elastic panels in an aircraft, executing a pull-up maneuver of given velocity and angular velocity, were derived by Sipcic and Morino [20]. The effect of the maneuver on the flutter speed and on the limit cycle amplitude was discussed for various load conditions. Meirovitch and Tuzcu [21, 22] have presented different works on simulating the motion of flexible aircrafts and derived some integrated approaches to control the complex maneuvering of an airplane. Two flight dynamics problems including the steady level cruise and a steady level turn maneuver were considered. The aeroelastic modeling and flutter characteristics of wing-stores configuration under different maneuvers was investigated by Fazelzadeh et al. [23, 24]. They have showed that the combination of flexible structural motion and maneuver parameters affects the flutter speed of the wing-stores configuration.

According to the best of the authors' knowledge the aeroelastic modeling and flutter analysis of aircraft wings containing an arbitrarily placed powered-engine and subjected to roll maneuver have not yet been addressed and will be presented in this study.

GOVERNING EQUATIONS

A schematic of a roll maneuvering aircraft wing-engine is presented in Fig. 1. Distances between the airplane center of gravity and the wing root, where the roll angular velocity acts, are clearly indicated in this figure. The wing typical section is represented in Fig. 1(b), where y_e and z_e are the distances between the center of gravity of the engine and the elastic axis of the wing. Also, points AE, AC, cg_w and cg_e refer to the wing elastic axes, aerodynamic center of the wing, wing center of gravity and engine center of gravity, respectively. Because of the wing complicated dynamic, several coordinate systems are used. The orthogonal axes X, Y, Z are fixed on the wing root. This coordinate system is called the un-swept wing coordinate system and rotates with respect to inertial frame at maneuver angular velocities. Another coordinate system is the swept wing coordinate system, *xyz*, in which the *x* axis lies along the length of the un-deformed wing. The last wing coordinate system is deformed wing coordinate system, $x'y'z'$, where x' lies along the deformed wing. After the wing deformation, the shear center of the cross-section located at x is displaced by an amount w in the z direction. Additionally, the angle of twist of the cross-section changes to θ about the *x* axis. This is because all equations will be expressed in *xyz* coordinate, but angular velocities of maneuvering airplane are expressed in X, Y, Z coordinate. It should be noted that while deriving the kinetic energy of the wing the angular velocity vector must be first transformed into the wing coordinate system. For swept wings *xyz* coordinate can be achieved from X,Y,Z by one rotation.

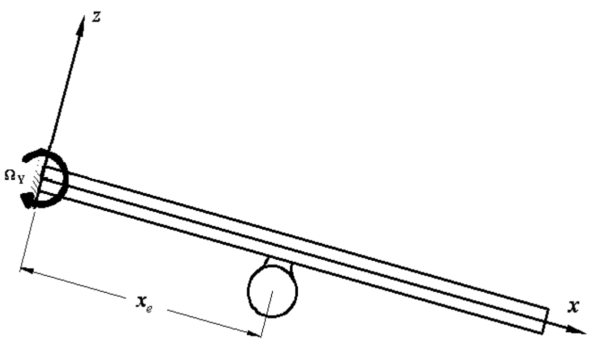

(a)

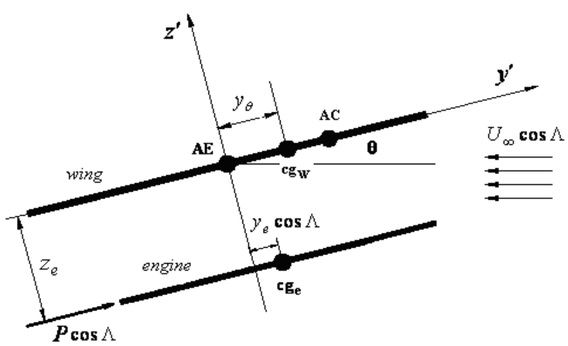

(b)

Fig. 1. (a) Schematic of the wing in rolling maneuver, (b) The wing typical section.

The transformation between X,Y,Z and x,y,z coordinate systems is

$$\begin{aligned} \hat{i} &= (\cos\Lambda)\hat{I} - (\sin\Lambda)\hat{J} \\ \hat{j} &= (\sin\Lambda)\hat{I} + (\cos\Lambda)\hat{J} \\ \hat{k} &= \hat{K} \end{aligned} \tag{1}$$

where $\hat{i},\hat{j},\hat{k}$ and $\hat{I},\hat{J},\hat{K}$ are the unit vectors of x,y,z and X,Y,Z coordinate systems, respectively. The transformation from x,y,z to $x'y'z'$ is given by [18]

$$\begin{aligned} \hat{i}' &= \hat{i} + w'\hat{k} \\ \hat{j}' &= \hat{j} + \theta\hat{k} \\ \hat{k}' &= -w'\hat{i} - \theta\hat{j} + \hat{k} \end{aligned} \tag{2}$$

The equations of motion are derived using Hamilton's variational principle that may be expressed as [25]

$$\int_{t_1}^{t_2} [\delta U - \delta T_w - \delta T_e - \delta W]dt = 0 , \tag{3}$$

$$\delta w = \delta\theta = 0 \quad \text{at} \quad t = t_1 = t_2$$

where U and T are strain energy and kinetic energy, and W is the work done by non- conservative forces. The indices w and e identify the wing and engine, respectively. The equations of motion for a wing-engine under roll maneuver are obtained as

$$\begin{aligned} & m\ddot{w} + EI_y w'''' + m x_a \ddot{\varphi} + (p\sin\Lambda\, w' H(x_e - x) + \\ & p\cos\Lambda\varphi' H(x_e - x) - p\cos\Lambda\varphi\delta(x - x_e))' + \\ & (pY_e \sin\Lambda\varphi' - p\cos\Lambda\varphi + p\sin\Lambda\, w')\delta(x - x_e) + \\ & C_{ww1}\Omega_y + C_{ww2}\Omega_y{}^2 + (M_e\ddot{w} + M_e\ddot{\varphi}\cos\Lambda\, Y_e - \\ & I_{\xi_e}\ddot{w}''\sin^2\Lambda - M_e\ddot{w}'' z_e{}^2 - M_e Y_e{}^2 \sin^2\Lambda\,\ddot{w}'' + I_{\xi_e}\ddot{\varphi}' \\ & \cos\Lambda\sin\Lambda - I_{\eta_e}\ddot{w}'' + M_e\ddot{\varphi}' Y_e{}^2 \cos\Lambda\sin\Lambda + \\ & C_{we1}\Omega_y + C_{we2}\Omega_y{}^2)\delta(x - x_e) - L = 0 \end{aligned} \tag{4}$$

$$\begin{aligned} & I_\alpha\ddot{\varphi} + m x_a \ddot{w} - GJ\varphi'' + pZ_e\cos\Lambda\delta(x - x_e) + \\ & p\cos\Lambda(x_e - x)w'' H(x_e - x) + C_{\varphi w1}\Omega_y + C_{\varphi w2}\Omega_y{}^2 \\ & + (I_\eta\ddot{\varphi} + I_\xi\cos^2\Lambda\ddot{\varphi} + M_e\ddot{\varphi}Z_e{}^2 + M_e\ddot{\varphi}\cos^2\Lambda\, Y_e{}^2 + \\ & M_e\ddot{w}Y_e\cos\Lambda - M_e\ddot{w}'\sin\Lambda\, Y_e{}^2\cos\Lambda - I_\xi\cos\Lambda\,\ddot{w}'\sin\Lambda \\ & C_{\varphi e1}\Omega_y + C_{\varphi e2}\Omega_y{}^2)\delta(x - x_e) - M = 0 \end{aligned} \tag{5}$$

where $C_{wwi}, C_{wei}, C_{\varphi wi}, C_{\varphi ei}$ are roll coefficients expressed in annex A. In Eqs. (4) and (5) the Heaviside and Dirac delta functions are used in order to accurately consider the location and properties of the thrust force and the attached mass, respectively, while the index e indicates the “engine” contributions. It should be noted here that the engine aerodynamic is not accounted for in governing equations.

The aerodynamic forces are derived from the finite-state aerodynamic model of Peters et al [26]. The wing sweep angle contribution is considered by appropriate modifications in aerodynamic model, the details are reported in [19]. Therefore, the modified Peter’s sectional lift and aerodynamic moment modified to account for the swept angle are

$$\begin{aligned} L = {} & \pi\rho_\infty b^2[-\ddot{w} + U_\infty\cos\Lambda\dot{\theta} - U_\infty\sin\Lambda\dot{w}' - \\ & ba(\ddot{\theta} + U_\infty\sin\Lambda\dot{\theta}')] + 2\pi\rho_\infty U_\infty b\cos\Lambda \\ & [-\dot{w} + U_\infty\cos\Lambda\theta - U_\infty\sin\Lambda\dot{w}' + b(\frac{1}{2} - a) \\ & (\dot{\theta} + U_\infty\sin\Lambda\theta') - \lambda_0] \end{aligned} \tag{6}$$

$$M = b(\frac{1}{2} + a)L - \pi\rho_\infty\, b^3[-\frac{1}{2}\ddot{w} + U_\infty \cos\Lambda\dot{\theta} - U_\infty \sin\Lambda \dot{w}' + b(\frac{1}{8} - \frac{a}{2})(\ddot{\theta} + U_\infty \sin\Lambda\dot{\theta}')] \tag{7}$$

where λ_0 is the induced-flow velocity. It should be noted that this model does not include drag force and it is assumed that drag effects are negligible.

SOLUTION METHODOLOGY

Due to intricacy of governing equations, it is difficult to get the exact solution. Therefore, in order to solve the above equations in a general way, the Galerkin's method is used [27]. To this end, w, θ are represented by means of series of trial functions, φ_i that should satisfy the boundary conditions, multiplied by time dependent generalized coordinates, $\mathbf{q_i}$.

$$w = \varphi_1{}^{\mathbf{T}}\mathbf{q_1} \qquad , \theta = \varphi_2{}^{\mathbf{T}}\mathbf{q_2} \tag{8}$$

Substituting Eqs. (6- 8) in Eqs. (4, 5) and applying the Galerkin procedure on these governing equations and using the orthogonal properties in the required integrations the following set of ordinary differential equations are obtained.

$$\mathbf{M}\ddot{\mathbf{q}} + \mathbf{C}\dot{\mathbf{q}} + \mathbf{K}\mathbf{q} = 0 \tag{9}$$

Herein, **M**, **C** and **K** denote the mass matrix, the damping matrix and the stiffness matrix, respectively, while **q** is the overall vector of generalized coordinates

$$\{\mathbf{q}\} = \left\{\mathbf{q_1}^{\mathbf{T}} \quad \mathbf{q_2}^{\mathbf{T}}\right\}^T \tag{10}$$

Six bending modes, six torsion modes, and six aerodynamic states are considered in the Galerkin method to transform Eqs. (4, 5) in a set of first-order coupled ordinary differential equations as

$$\dot{\mathbf{Z}} = [\mathbf{A}]\,\mathbf{Z} \tag{11}$$

The state vector $\mathbf{Z}$ is defined as

$$\mathbf{Z} = \left\{\boldsymbol{\lambda}^{\mathbf{T}}\ \mathbf{q}^{\mathbf{T}}\ \dot{\mathbf{q}}^{\mathbf{T}}\right\}^{\mathbf{T}} \tag{12}$$

where $\boldsymbol{\lambda}$ is the vector of induced flow states and the system matrix [**A**] has the form

$$[\mathbf{A}] = \begin{bmatrix} [\mathbf{0}] & [\mathbf{I}] \\ -[\mathbf{M}]^{-1}[\mathbf{K}] & -[\mathbf{M}]^{-1}[\mathbf{C}] \end{bmatrix} \tag{13}$$

The problem is now reduced to the classical eigenvalue solution, to find the eigenvalues of matrix $[\mathbf{A}]$ for a given values of the air speed parameter U_∞. The eigen-value ω is a continuous function of the air speed U_∞. For $U_\infty \neq 0$, ω is in general complex, $\omega = \mathrm{Re}(\omega) + i\,\mathrm{Im}(\omega)$. When $\mathrm{Re}(\omega) = 0$ and $\mathrm{Im}(\omega) \neq 0$ the wing is said to be in critical flutter condition. At some point, as U_∞ increases, $\mathrm{Re}(\omega)$ turns from negative to positive so that the motion turns from asymptotically stable to unstable.

NUMERICAL RESULTS

The classical Goland's wing extended to variable wing sweep angles is considered. Pertinent data for this particular wing are

$$m = 35.695\,\text{kg/m},\ l = 6.1\,\text{m},\ b = 0.915\,\text{m},$$
$$EI_y = 9.765{*}106\,\text{N.m}^2, I_{M_e} = 20\,\text{kg.m},$$
$$GJ = 0.989{*}106\,\text{N.m}^2,\ a = -0.34,$$
$$mk_m{}^2 = 8.694\,\text{kg.m},\ x_\theta = 0.183\text{m},$$

Also, the following nondimensional parameters are made,

$$P = \frac{pl^2}{\sqrt{GJEI_y}},\ v_f = \frac{U_f}{b\omega_\theta},\quad X_e = \frac{x_e}{l},$$
$$Y_e = \frac{y_e}{b},\ Z_e = \frac{z_e}{b},\ \eta_e = \frac{M_e}{ml},\ \Omega y = \frac{\Omega_y}{\omega_\theta},$$
$$\overline{R}_X = \frac{R_X}{b},\ \overline{R}_Z = \frac{R_Z}{b}$$

In Table 1, for the purpose of model validation, the results for the swept wing without external mass are compared with Karpouzian and Librescu [29] and good agreement is reported in the range of $-10 < \Lambda < 30$. For other ranges small differences come from the fact that the Peter's model is used here while in [29] the Theodorsen's model was used. It can be seen from this Table that both backward and forward sweep angles increase the flutter speed, significantly.

In addition, in the absence of the external mass and sweep, comparisons are also made with [17], in Fig. 2. There are some differences between the present results and those in [17] associated with the fact that the Galerkin method is used here while the finite element method was used by them in the solution procedure. The same wing characteristics used in this reference are selected for model validation. In this figure the flutter boundary for a clean straight wing subjected to a lateral follower force is illustrated. A continued decrease in the flutter speed accompanying the increase in the follower force is seen. Clearly an increase in the magnitude of the follower force is destabilizing and leads to instability at lower speeds.

Table 1 Validation of the non-dimensional flutter speed for a swept clean wing

Wing sweep angle (deg)	Ref. [9]	Present	Error (%)
-30	13.3	12.31	7.4
-20	12	11.5	4
-10	11.2	11	1.7
0	10.8	10.77	0.2
10	10.9	10.84	0.5
20	11.3	11.2	0.8
30	11.9	11.8	0.8

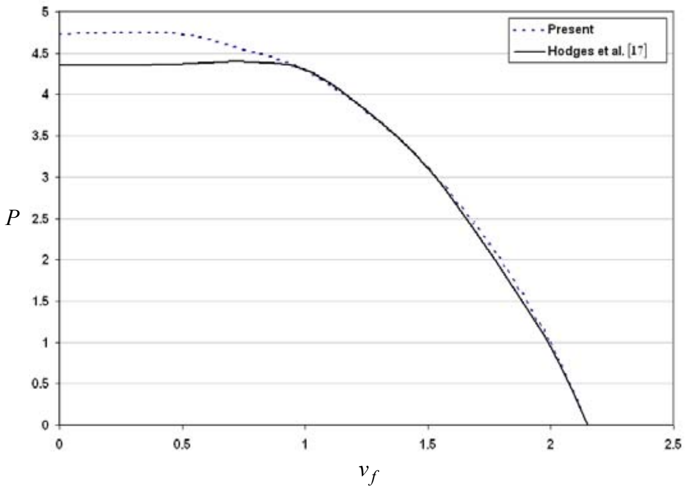

Fig. 2. The flutter boundary for an un-swept clean wing subjected to thrust force

Figure 3 shows the variation of the flutter speed and frequency of a clean wing for selected values of the roll angular velocity due to variations in the wing sweep angle. It can be seen from this figure that both flutter speed and frequency significantly decrease by increasing the roll angular velocity. Furthermore, both backward and forward sweep angles improve the stability domain of the wing. The trend in these figures is similar to the one reported in [5, 6].

Figure 4 shows a parametric study investigating the effect of the roll angular velocity on the flutter boundary for the wing carrying a powered engine. The wing is considered to have a sweep angle of $\Lambda = 30$. Furthermore, the engine is considered to have $\eta_e = 0.5$ and located at $X_e = 0.5$, $Y_e = -0.25$. There is a continuous decrease in the magnitude of the thrust required for instability with an increase in airspeed. This happens because the destabilizing effect of the aerodynamic forces is added to the system, leading to instability at lower levels of the follower force. Also, it is clear that increasing the roll angular velocity constricts the stability domain of the wing-engine, significantly. This is more obvious for higher values of the roll maneuver angular velocities.

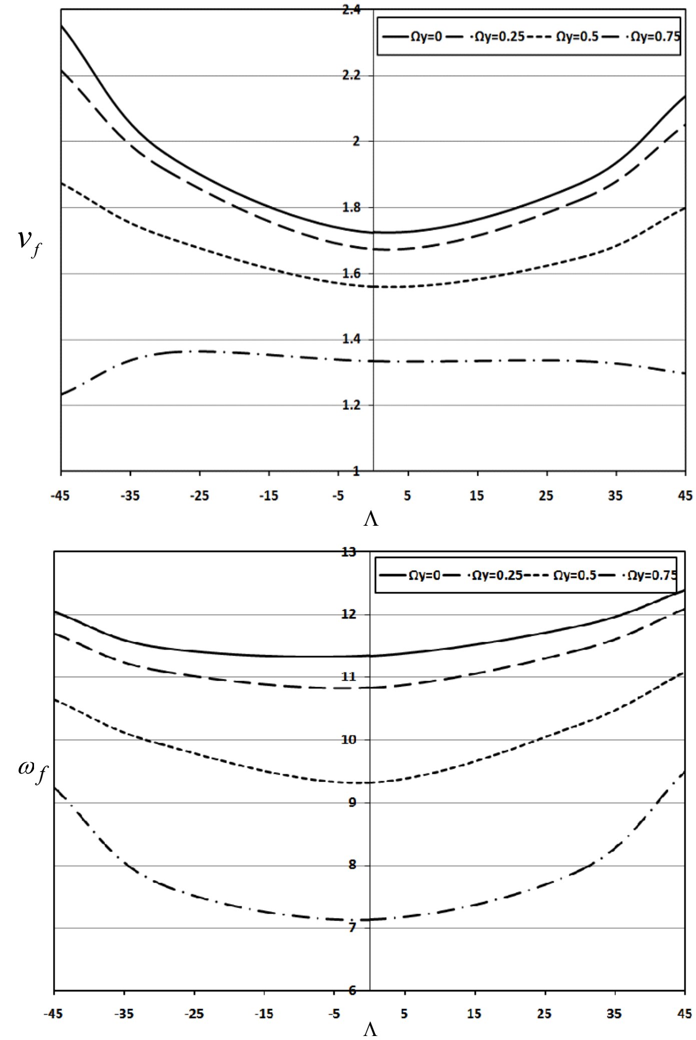

Fig. 3. Effects of the sweep angle on the clean wing flutter boundary for selected values of roll angular velocities:(a) Flutter speed, (b) Flutter frequencies

Figures 5-7 show the influence of the spanwise location of the engine on the flutter speed and frequency of the wing for different design parameters. In these figures, the engine is considered to have $\eta_e = 0.5$ and located at $Y_e = -0.25$. Figure 3 shows the variation of the flutter speed and frequency of the wing for selected values of the roll angular velocity due to variations in the spanwise location of the external mass. The wing sweep angle is $\Lambda = 30$ deg and the engine thrust is $P = 2$ in this case.

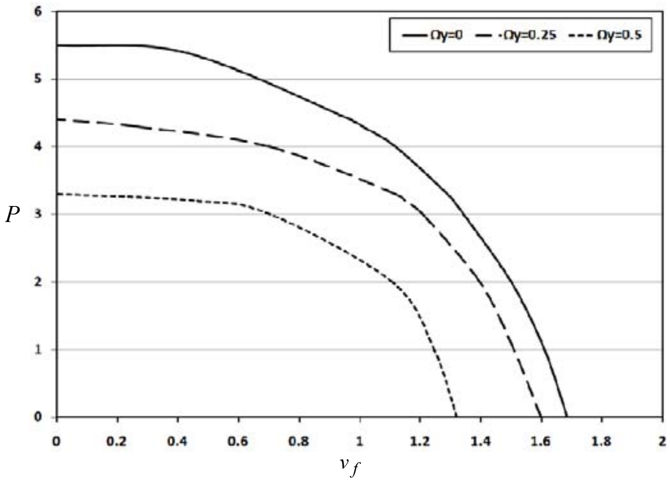

Fig. 4. Effect of the maneuver angular velocity on the wing flutter boundaries for $\eta_e = 0.5$, $X_e = 0.5$, $Y_e = -0.25$ and $\Lambda = 30$ deg.

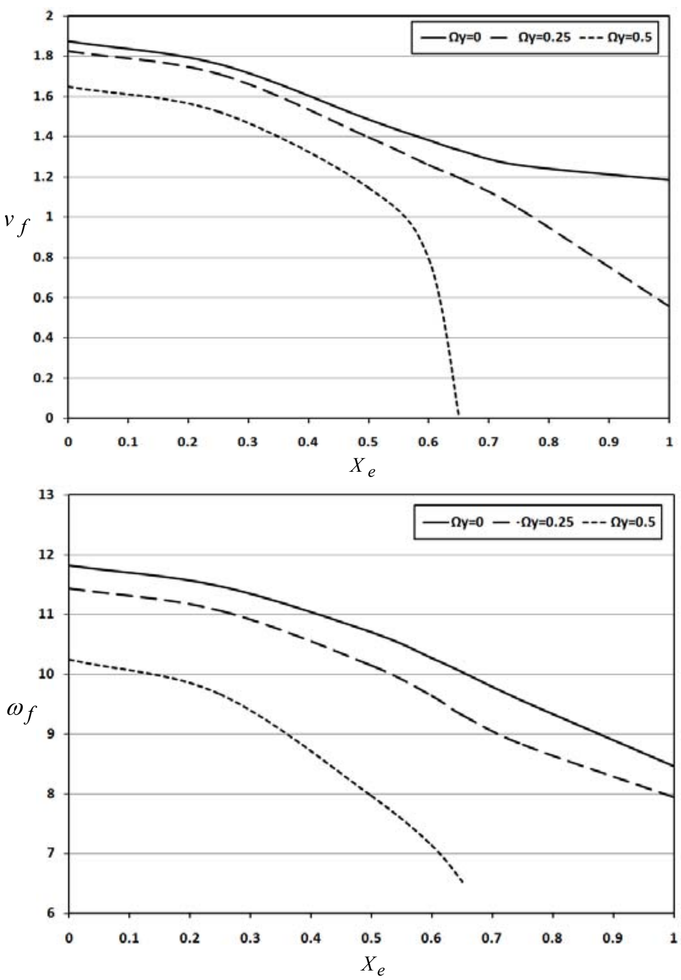

Fig. 5. Effects of the spanwise position of the engine on the wing flutter boundary for selected values of roll angular velocities and for $Y_e = -0.25$, $\eta_e = 0.5$, $\Lambda = 30$ deg and $P = 2$:(a) Flutter speed, (b) Flutter frequencies.

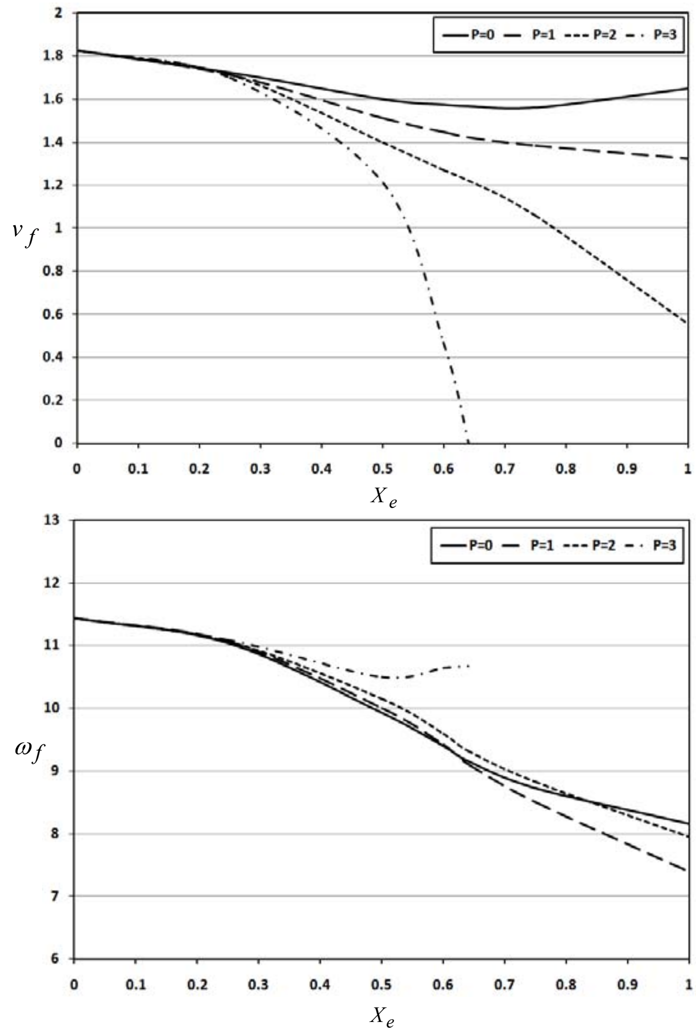

Fig. 6. Effects of the spanwise position of the engine on the wing flutter boundary for selected values of thrust forces and for $Y_e = -0.25$, $\eta_e = 0.5$, $\Lambda = 30$ deg and $\Omega_y = 0.25$:(a) Flutter speed, (b) Flutter frequencies.

The effect of the roll angular velocity on the wing flutter speed is clearly highlighted. The results show that an increase of roll angular velocity can induce a lower flutter speed. This means that rolling maneuver decreases the maneuvering ability of the airplane. For large values of the roll angular velocity the diagram coincides with zero-velocity line when the engine is located toward the wing tip. This means that rolling maneuver may lead to instability even in the absence of the air flow.

Figure 6 demonstrates the effect of the spanwise location of the powered-engine on the wing flutter boundary for the selected values of the thrust force. The wing sweep angle is $\Lambda = 30$ deg and the maneuvering aircraft is considered with $\Omega_y = 0.25$. In the absence of the engine thrust, the lowest value of the flutter speed is around $X_e = 0.7$. There is a marked difference between this result and one obtained for nonmaneuvering aircraft. For the case of the wing with a mounted engine, it can be seen that increasing the distance of the engine from the wing root will decrease the flutter speed. This is more apparent for greater values of the engine thrust.

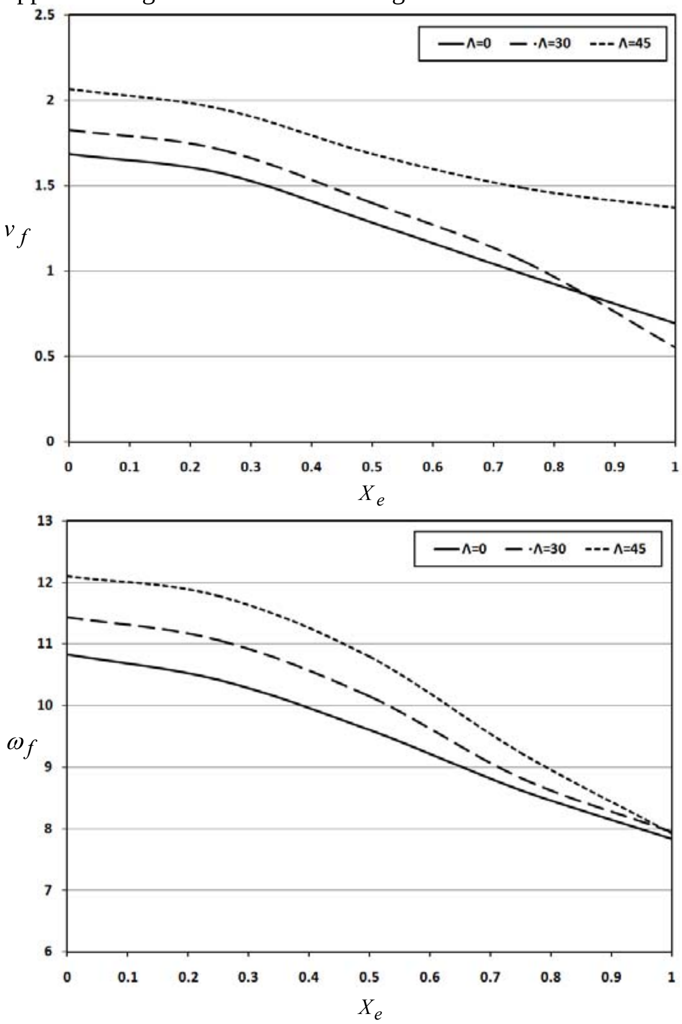

Fig. 7. Effects of the spanwise position of the engine on the wing flutter boundary for selected values of the wing sweep angle and for $Y_e = -0.25$, $\eta_e = 0.5$, $P = 2$ and $\Omega_y = 0.25$: Flutter speed, (b) Flutter frequencies.

The flutter speed drops to zero for large values of the engine thrust when the engine is located toward the wing tip. This can be qualitatively explained as the increase of the destabilizing effect of the engine mass and thrust leading to instability, even at zero air speed.

Effects of the spanwise location of the engine on the wing stability region for selected values of the wing sweep angle are shown in Fig. 7. The engine thrust is again $P = 2$ and the maneuvering aircraft is considered with $\Omega_y = 0.25$. Results indicate that the engine mounting location considerably affects the dynamic stability of the wing. It can be seen in Fig. 7(a) that increasing the distance of the engine from the wing root will decrease the flutter speed. Figure 7(b) also reveals that the flutter frequency drops by moving the engine towards the wing tip. In addition, effects of the wing sweep angle on the wing flutter speed and frequency is highlighted. Results show continued increase of flutter speed and frequency with increased sweep angle. This means that the wing sweep angle could positively affect the aeroelastic performance of the wing.

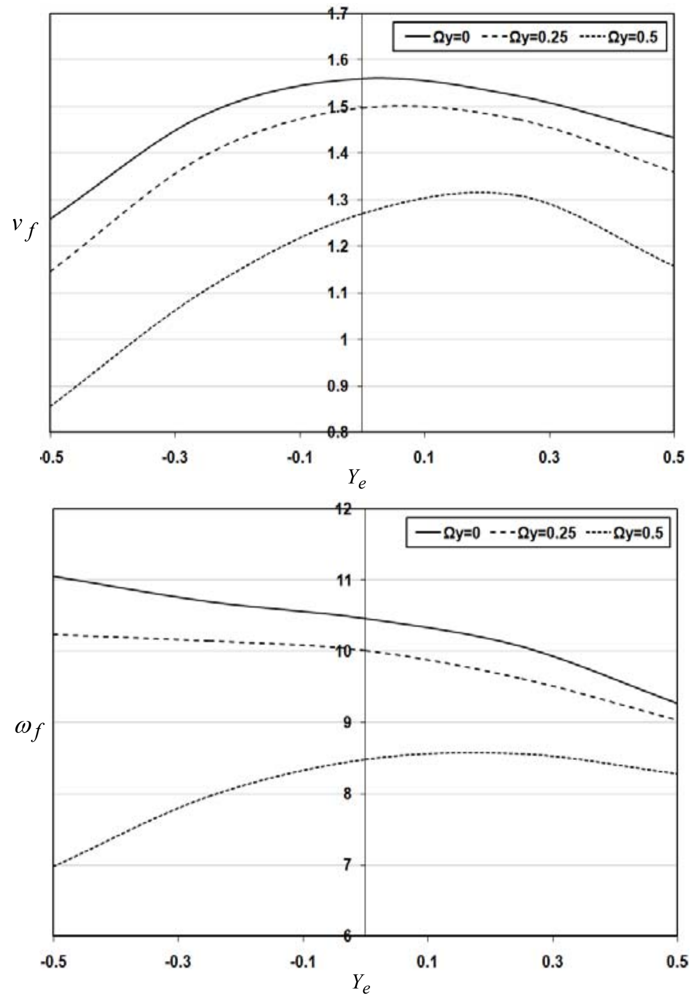

Fig. 8. Effects of the chordwise position of the engine on the wing flutter boundary for $X_e = 0.5$, $\Lambda = 30$ deg, $P = 2$ and $\eta_e = 0.5$ a) Flutter speed, (b) Flutter frequencies.

Figure 8 demonstrates the influence of the chordwise location of the engine on flutter speed and the frequency of the wing for different values of the roll maneuver angular velocity. The engine is located at the middle of the wing span and considered to have $\eta_e = 0.5$. Moreover, the wing sweep angle is $\Lambda = 30$ deg and the engine thrust is $P = 2$. It can be seen that the engine chordwise location contributes considerably on the wing-engine stability. When the engine is located toward the leading edge of the wing there is an increases the flutter speed, in the case of the wing carrying the engine without the follower force. However, it is evident that the flutter speed decreases in both positive and negative region of the diagram due to the presence of the follower force on the engine. Indeed, increasing the distance of the engine from the wing elastic axes in chordwise direction increases the destabilizing effects of the follower force and consequently decreases the flutter speed. Although, this is true for all values of the roll angular velocity, the stability domain is dramatically restricted by increasing the maneuver angular velocity. Furthermore, as is shown in Fig. 8(b), when the engine is located toward the leading edge of the wing the flutter frequency decreases for normal maneuvering angular velocities. This behavior is dependent, obviously, on the value of the roll angular velocity. For higher values of the maneuvering angular velocities different behaviors can be seen in both flutter speed and frequency diagram.

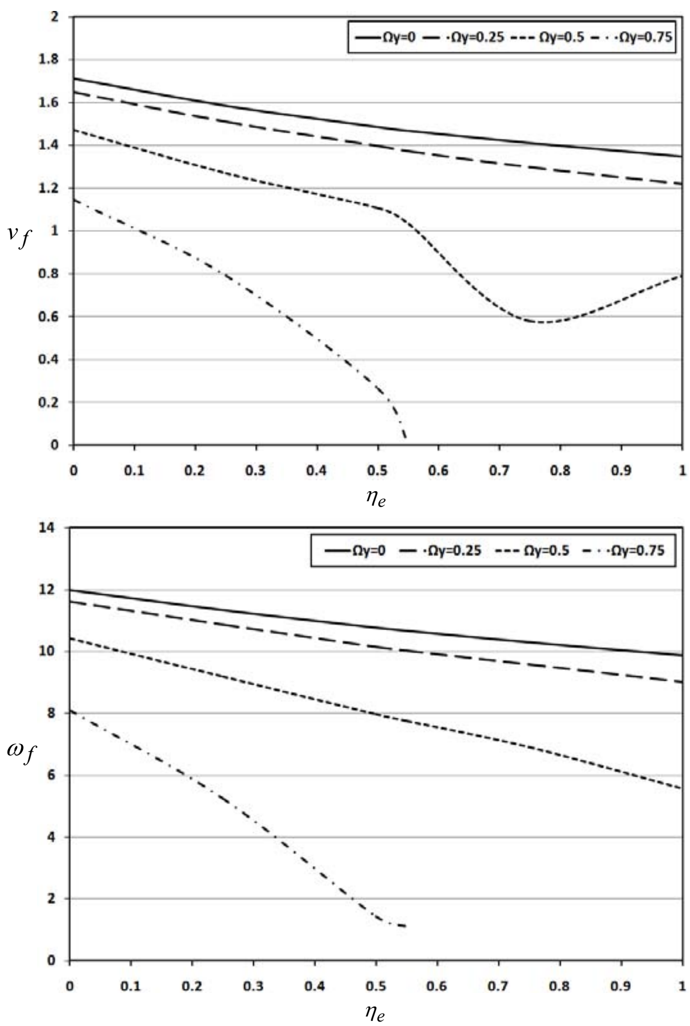

Fig. 9. Effects of the engine mass ratio on the wing flutter boundary for $X_e = 0.5$, $Y_e = -0.25$ and $P = 2$:(a) Flutter speed, (b) Flutter frequencies.

Figures 9 shows the effects of the engine mass on the flutter speed and frequency of the swept wing for different roll angular velocity values. The engine is located at the middle of the wing span and $Y_e = -0.25$. Also, the wing sweep angle is $\Lambda = 30$ deg and the engine thrust is $P = 2$. Results show that the engine mass decreases the flutter speed and plays a destabilizing role in the dynamic stability of the wing. For high roll angular velocity values, increasing the engine mass may lead to instability at zero air speed. This means that increasing the engine mass increases the destabilizing effects of the roll maneuver. Furthermore, the effects of the roll angular velocity on the wing flutter speed and frequency can be observed in this figure. As expected, by increasing the roll angular velocity both the flutter speed and the flutter frequency of the wing decrease.

CONCLUSIONS

The effect of the rolling maneuver, one of the most popular flight maneuvers, on flutter of an airplane wing carrying an arbitrary placed powered-engine is considered. The governing equations include effects of both maneuver induced and lift and aerodynamic moment induced forces. Results are indicative of the important influence of the roll angular velocity on flutter speed and frequency of the wing-engine. The results show that the rolling maneuver has a detrimental effect on the dynamic flutter and restricts the wing dynamic stability region. Because of the destabilizing effect of the maneuver induced forces, dependent to wing-engine characteristics, for large values of the roll angular velocity, the flutter may take place at zero air velocity. On the other hand, increasing the rolling moment always seems to lower the flutter frequency. Furthermore, The engine parameters, such as η_e, X_e, Y_e and also the engine thrust, acts as a transverse follower force, causing remarkable changes in the wing-engine flutter speed and frequency. Clearly the effect of the roll angular velocity on the flutter speed is strongly dependent to the engine mass and its location. It is found that the flutter speed and frequency in the case of a heavy store is lower than those obtained for a light one, independent of the maneuver conditions.

NOMENCLATURE

b	=	Wing semi chord
E	=	Young's modulus
G	=	Shear modulus
H	=	Heaviside function
I	=	Wing cross-section moment of inertia
J	=	Wing cross-section polar moment of inertia
$\hat{\mathbf{I}}, \hat{\mathbf{J}}, \hat{\mathbf{K}}$	=	Unit vectors of un-swept coordinate system
$\hat{\mathbf{i}}, \hat{\mathbf{j}}, \hat{\mathbf{k}}$	=	Unit vectors of un-deformed wing coordinate system

$\hat{\mathbf{i}}', \hat{\mathbf{j}}', \hat{\mathbf{k}}'$	=	Deformed wing coordinate unit vectors
l	=	Wing length
k_m	=	Mass radius of gyration of wing cross-section
L, M	=	Wing sectional lift and moment
m	=	Mass of the wing per unit length
M_e	=	Engine mass
P	=	Non-dimensional follower force
$\mathbf{R_e}$	=	Engine displacement vector
T	=	Kinetic energy
U	=	Strain energy
U_∞	=	Air stream velocity
v_f	=	Non-dimensional flutter speed
w	=	Displacement in z direction
W	=	Work done by non-conservative forces
X, Y, Z	=	Base coordinate system
x, y, z	=	Undeformed swept wing coordinate system
x', y', z'	=	Deformed wing coordinate system
X_e, Y_e, Z_e	=	Nondimensional engine location in x, y and z directions, respectively
y_θ	=	Distance between center of gravity and elastic axis of the wing
δ	=	Variational operator
δ_D	=	Dirac delta function
η, ξ	=	Wing cross-section local coordinates
η_e	=	Nondimensional engine mass
Λ	=	Wing sweep angle
λ_n	=	Induced flow states
θ	=	Twist angle
ρ	=	Wing material density
ρ_∞	=	Air density
Ω_y	=	Non-dimensional roll angular velocity
ω_f	=	Flutter frequency
ω_θ	=	Torsional frequency

REFERENCES

[1] Goland, M., 1945, "The flutter of a uniform cantilever wing," Journal of Applied Mechanics, Vol. 12, pp. 197-208.
[2] Goland, M. and Luke, Y.L., 1948, "The flutter of a uniform wing with tip weights," Journal of Applied Mechanics, Vol. 15, pp. 13-20.
[3] Harry L.R. and Charles E.W., 1949, "Flutter of a uniform wing with an arbitrarily placed mass according to a differential equation analysis and a comparison with experiment," NASA Technical Report, NACA TN-1848.
[4] Lottati, I., 1987, "Aeroelastic stability characteristics of a composite swept wing with tip weights for an unrestrained vehicle, Journal of Aircraft," Vol. 24, pp. 793-802.
[5] Gern, H. and Librescu, L., 1998, "Effect of externally mounted stores on aeroelasticity of advanced aircraft wings," Journal of Aerospace Science and Technology, Vol. 5, pp. 321-333.
[6] Gern, H. and Librescu, L., 1998, "Static and dynamic aeroelasticity of advanced aircraft wings carrying external stores," AIAA Journal, Vol. 36, pp. 1121-1129.
[7] Na, S. and Librescu, L., 2000, "Dynamic response of adaptive cantilevers carrying external stores and subjected to blast loading," Journal of Sound and Vibration, Vol. 231, pp. 1039-1055.
[8] Librescu, L. and Song, O., 2008, "Dynamics of composite aircraft wings carrying external stores," AIAA Journal, Vol. 46, pp. 568, 572.
[9] Bolotin, V.V., 1963, Non-Conservative Problems of the Theory of Elastic Stability, Pergamon Press, Oxford.
[10] Bolotin, V. V. and Zhinzher, N. I., 1969, "Effects of damping on stability of elastic systems subjected to non-conservative forces," International Journal of Solids and Structures, Vol. 5, pp. 965-989.
[11] Kalmbach, C. F., Dowell, E. H. and Moon, F. C., 1974, "The suppression of a dynamic instability of an elastic body using feedback control," International Journal of Solids and Structures, Vol. 15, pp. 10-36.
[12] Zuo, Q. H. and Schreyer, H. L., 1996, "Flutter and divergence instability of non-conservative beams and plates," International Journal of Solids and Structures, Vol. 33, pp. 1355-1367.
[13] Detinko, F. M., 2002, "Some phenomena for lateral flutter of beams under follower load," International Journal of Solids and Structures, Vol. 39, pp. 341-350.
[14] Como, M., 1966, "Lateral buckling of a cantilever subjected to a transverse follower force," International Journal of Solids and Structures, Vol. 2, pp. 515-523.
[15] Feldt, W. T. and Herrmann, G., 1974, "Bending-Torsional flutter of a cantilevered wing containing a tip mass and subjected to a transverse follower force," Journal of the Franklin Institute, Vol. 297, pp. 467-478.
[16] Hodges, D. H., 2001, "Lateral-Torsional flutter of a deep cantilever loaded by a lateral follower force at the tip," Journal of sound and vibration, Vol. 247, pp. 175-183.

[17] Hodges, D. H., Patil, M. J. and Chae, S., 2002, "Effect of thrust on bending-torsion flutter of wings," Journal of Aircraft, Vol. 39, pp. 371-376.

[18] Fazelzadeh, S.A., Mazidi, A. and Kalantari, H., 2009, "Bending-Torsional flutter of wings with an attached mass subjected to a follower force," Journal of Sound and Vibration, Vol. 323, pp. 148-162.

[19] Mazidi, A. and Fazelzadeh, S. A., 2010, "The flutter of a swept aircraft wing with a powered-engine," Journal of Aerospace Engineering, In press.

[20] Sipcic, S.R. and Morino, L., 1991, "Dynamic behavior of the fluttering two-dimensional panels on an airplane in pull-up maneuver," AIAA Journal, Vol. 29, pp. 1304, 1312.

[21] Meirovitch, L. and Tuzcu, I., 2001, "Multidisciplinary approach to the modeling of flexible aircraft," International Forum on Aeroelasticity and Structural Dynamics, Madrid/Spain, pp. 435-448.

[22] Meirovitch, L. and Tuzcu, I., 2003, "Integrated approach to the dynamics and control of maneuvering flexible aircraft," NASA, CR-2003-211748.

[23] Fazelzadeh, S. A., Mazidi, A., Rahmati, A. R. and Marzocca, P., 2009, "The effect of multiple stores arrangement on flutter speed of a shear deformable wing subjected to pull-up angular velocity," Aeronautical Journal, Vol. 113, pp. 661-668.

[24] Fazelzadeh, S. A., Marzocca, P., Rashidi, E. and Mazidi, A., 2010, "Effects of rolling maneuver on divergence and flutter of aircraft wings carrying an external store," Journal of Aircraft, Vol. 47, pp. 64-70.

[25] Baruh, H., 1999, Analytical Dynamics, McGraw-Hill, Boston.

[26] Peters, D.A., Karunamoorthy, S. and Cao, W.M., 1995, "Finite state induced flow models; part i: two-dimensional thin airfoil," Journal of Aircraft, Vol. 32, pp. 313-322.

[27] Fletcher, C.A.J., 1984, Computational Galerkin methods, Springer-Verlag, New York.

[28] Hodges, D.H. and Pierce, G.A., 2002, Introduction to Structural Dynamics and Aeroelasticity, Cambridge University Press, Cambridge.

[29] Karpouzian, C. and Librescu, L., 1996, "Non-Classical effects on divergence and flutter of anisotropic swept aircraft wings," AIAA Journal, Vol. 34, pp. 786-794.

ANNEX A

$$C_{ww1} = 0$$

$$\begin{aligned} C_{ww2} = {} & m \sin^2\Lambda\, w - m\cos^2\Lambda\, w + m\cos^2\Lambda\, w''\, k m_1{}^2 - \\ & m\cos\Lambda\sin\Lambda\,\varphi'\, k m_2{}^2 + m\cos\Lambda\sin\Lambda\,\varphi'\, k m_1{}^2 + \\ & m x_a \sin^2\Lambda\,\varphi - \cos^2\Lambda\, m x_a\,\varphi \end{aligned}$$

$$\begin{aligned} C_{we1} = {} & 2M_e\sin\Lambda\,\dot{\varphi} Z_e + 2M_e\sin^2\Lambda\,\dot{\varphi}' Z_e Y_e + \\ & 2M_e\cos^2\Lambda\,\dot{\varphi}' Y_s Z_s + 4M_e\cos\Lambda\,\dot{w}' Z_e \end{aligned}$$

$$\begin{aligned} C_{we2} = {} & -M_e\sin^2\Lambda\,\varphi\cos\Lambda\, Y_e - M_e\cos^3\Lambda\,\varphi Y_e - \\ & M_e\cos^3\Lambda\sin\Lambda\, Y_e{}^2\varphi' - M_e\cos^3\Lambda\, x_e\varphi' Y_s - \\ & I_{\xi e}\cos^3\Lambda\sin\Lambda\,\varphi' - I_{\xi_e}\sin^3\Lambda\,\varphi'\cos\Lambda - \\ & M_e\sin^3\Lambda\cos\Lambda\, Y_e{}^2\varphi' - I_{\eta e} w''\sin^2\Lambda + \\ & I_{\xi e}\sin^4\Lambda\, w'' + M_e\cos^2\Lambda\sin^2\Lambda\, Y_e{}^2 w'' + \\ & M_e\cos\Lambda\sin\Lambda\,\varphi' Z_e{}^2 + M_e\cos^2\Lambda\, x_e w'' \\ & \sin\Lambda\, Y_e + M_e\sin^4\Lambda\, w'' Y_e{}^2 - M_e\sin^2\Lambda \\ & Z_e{}^2 w'' - M_e\sin^2\Lambda\, Z_e - M_e\cos^2\Lambda\, Z_e - \\ & M_e\sin^2\Lambda\, w - M_e\cos^2\Lambda\, w + I_{\eta e}\cos\Lambda\sin\Lambda\,\varphi' \end{aligned}$$

$$C_{\varphi w1} = 0$$

$$\begin{aligned} C_{\varphi w2} = {} & -I_\alpha\varphi + m x_a\cos^2\Lambda\, w + mkm_2{}^2\sin\Lambda\cos\Lambda\, w' - mkm_1{}^2 \\ & \sin\Lambda\cos\Lambda\, w' + 2mkm_2{}^2\sin^2\Lambda\,\varphi - 2mkm_1{}^2\sin^2\Lambda\,\varphi \\ & - mkm_2{}^2\cos^2\Lambda\,\varphi + mkm_1{}^2\cos^2\Lambda\,\varphi \end{aligned}$$

$$\begin{aligned} C_{\varphi e1} = {} & 2M_e\cos^2\Lambda\,\dot{w}' Z_e Y_e + 2M_e\sin^2\Lambda\,\dot{w}' Y_e Z_e - \\ & 2M_e\sin\Lambda\,\dot{w} Z_e \end{aligned}$$

$$\begin{aligned} C_{\varphi e2} = {} & -M_e\sin^2\Lambda\cos^2\Lambda\, Y_e{}^2\varphi - I_\xi\varphi\cos^2\Lambda\sin^2\Lambda + \\ & M_e\cos^3\Lambda\, x_e w' Y_e + M_e\cos^3\Lambda\sin\Lambda\, Y_e{}^2 w' - \\ & I_\eta\sin\Lambda\cos\Lambda\, w' - M_e\sin^2\Lambda\cos\Lambda\, Y_e Z_e + \\ & I_\eta\varphi\cos^2\Lambda - M_e\sin^2\Lambda\, w Y_e\cos\Lambda - M_e\cos^3\Lambda\, w Y_e \\ & - M_e\sin\Lambda\cos\Lambda\, w' Z_e{}^2 + I_\xi\cos\Lambda\sin^3\Lambda\, w' + \\ & I_\xi w'\cos^3\Lambda\sin\Lambda - M_e\cos^3\Lambda\, Z_e Y_e + M_e\sin^3\Lambda \\ & w' Y_e{}^2\cos\Lambda - M_e\cos^4\Lambda\,\varphi Y_e{}^2 + M_e\cos^2\Lambda\, Z_e{}^2\varphi \\ & - I_\xi\cos^4\Lambda\,\varphi + M_e\sin\Lambda\cos^2\Lambda\, Y_e x_e\varphi + \\ & M_e\sin\Lambda\cos\Lambda\, Z_e x_e \end{aligned}$$